ELSEVIER

Journal of Chromatography A, 874 (2000) 131–142

JOURNAL OF CHROMATOGRAPHY A

www.elsevier.com/locate/chroma

# Analytical magnetapheresis of magnetically susceptible particles

C. Bor Fuh*, L.Y. Lin, M.H. Lai

*Department of Applied Chemistry, Chaoyang University of Technology, 168 Gifeng East Road, Wufeng, Taichung County 413, Taiwan*

Received 8 October 1999; received in revised form 28 December 1999; accepted 11 January 2000

**Abstract**

Analytical magnetapheresis is a newly developed technique for analyzing magnetic particles. The magnetically susceptible particles form deposition patterns after flowing through a separation channel in a magnetic field. The separation channel requirements for analytical magnetapheresis are an excellent seal for the carrier flow and ease of disassembly after magnetapheresis. Previously used separation channels often exhibit variable channel leakage and unstable flow velocities. We improved the separation channel assembly to ensure stable, high flow velocities and characterized the system with various magnetically susceptible and labeled particles. Our new separation channel featured silicone sealant with embedded nylon wires and met analytical magnetapheresis requirements. Characterization of this system was performed using several magnetically susceptible particles, and we studied a variety of diamagnetic sample labels with paramagnetic ions and magnetically susceptible particles at different flow-rates and solution pH values. The minimal labeling concentration for complete deposition was determined to be approximately $2.50 \cdot 10^{10}$ ions per particle for test samples at a flow velocity of 0.67 mm $s^{-1}$ and a magnetic field gradient of 2.8 T $mm^{-1}$. Silicas, yeasts and blood cells were used for these studies. We determined that the minimal difference in magnetic susceptibility ($\Delta\chi$) for successful separation was approximately $2.00 \cdot 10^{-6}$ [SI]. The magnetic susceptibilities of Dynabeads M-450 at several separation distances and flow-rates were determined to be 0.25 [SI], within 2% of values published by other workers. The magnetic susceptibilities of various ion-labeled yeasts and cells were determined and most varied by less than 5% at different flow-rates. The results of this study provide very important references for analytical magnetapheresis applications. 

*Keywords:* Magnetapheresis; Magnetic particles

## 1. Introduction

Magnetic separation has been widely used in the manufacturing and mining industries since the nineteenth century [1,2]. Magnetic separation and related techniques for use in biotechnology [3–9], wastewater treatment [10,11] and other applications [12] have grown rapidly in recent years. The advantages of magnetic separation are that it is simple, fast and selective. Magnetic separation using permanent magnets is especially economical and deserves further development.

Analytical magnetapheresis is a newly developed technique for analyzing magnetic particles [3]. Magnetically susceptible particles in carriers flow through thin (<0.05 cm), ribbon-like separation channels

*Corresponding author. Tel.: +886-4-3323-000 (ext. 4306); fax: +886-4-3742-341.

*E-mail address:* cbfuh@mail.cyut.edu.tw (C.B. Fuh)

0021-9673/00/$ – see front matter 
PII: S0021-9673(00)00074-1

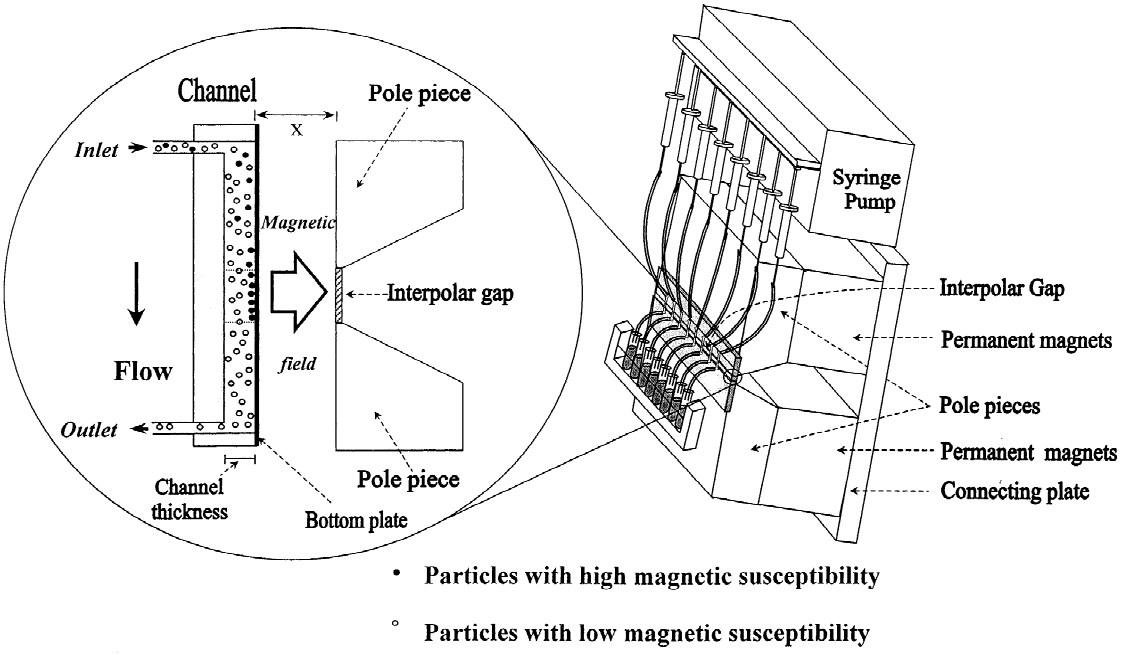


Fig. 1. General schematic of the analytical magnetapheresis system with multiple channels.

within magnetic fields and form deposition patterns on the channel bottom plate, as shown in Fig. 1. The magnetic forces act perpendicular to the channel flow axis and toward interpolar gap directions. Particles with high magnetic susceptibility (shown as solid circles in the figure) are attracted by the magnetic forces and deposited upon the interpolar gap as they pass along the separation channel. Diamagnetic particles and those with low magnetic susceptibility (shown as hollow circles in the figure) are relatively less affected by the magnetic forces and pass completely through the separation channel. Therefore, particles with different magnetic susceptibilities are separated during passage through the separation channel. The forces acting on samples can be calculated with good accuracy since the separation channel is unpacked and has a simple geometry. Deposition patterns of magnetically susceptible particles were calculable from the principle with known sample physical parameters. One such physical parameter could be deduced from the percentage of particle depositions.

The separation channel requirements for analytical magnetapheresis were: an excellent seal for channel flows, and ease of disassembly after magnetapheresis. The latter requirement was required for convenient examination and preservation of deposited materials. The typical separation channel of analytical magnetapheresis previously used a silicone rubber spacer sandwiched between the top and bottom plates for easy opening. The drawbacks of the previously used separation channel are variable channel leakage and unstable flow velocities. We built a new magnetic separator to eliminate these drawbacks. The new separator was tested with various magnetic particles, labeled particles, and cells at various flow-rates and solution pH values. The optimization of labeled particles and cells for analytical magnetapheresis were also surveyed.

## 2. Theory

The theory behind calculation of sample magnetic susceptibilities from percentages of samples retrieved at the outlet has been described in the literature [3]. Here, we give only a brief summary. It may be assumed that particles move quasistatically (without inertial effects) within the aqueous medium, and particle motion may be described by considering the

viscous force, $F_d$, to be equal to the magnetic force, $F_m$.

Dimensionless number, $\zeta$, groups the material and geometric constants of the magnetic deposition system for easy comparison of different systems. Fractional retrieval of particle, $\epsilon$, indicates the percentages of injected samples exit at outlet in analytical magnetapheresis. The dimensionless parameters, $\zeta$ and $\epsilon$, are defined as follows for convenience.

$$\zeta = \frac{1}{9} \cdot \frac{r^2}{\eta v_{max}} \cdot \frac{\Delta\chi}{\mu_0} \cdot \frac{B_0^2}{a} \quad (1)$$

$$\epsilon = \frac{N_{out}}{N_{in}} \quad (2)$$

where $B_0$ is the saturation field inside the interpolar gap, $a$ is half the interpolar gap width, $v_{max}$ is the maximum linear carrier flow velocity, $\eta$ is carrier viscosity, $r$ is the particle radius, $\Delta\chi$ is the effective particle magnetic susceptibility (difference in magnetic susceptibilities between particles and carriers), $\mu_0$ is the magnetic permeability of the vacuum, $\epsilon$ is the fractional retrieval of the particles, $N_{in}$ is the number of particles entering at the channel inlet, and $N_{out}$ is the number of particles exiting at the channel outlet. Particle trajectories in the magnetic fields can be obtained using Maple software with suitable equations [3]. Theoretical retrieval, $\epsilon_{th}$, can be determined using the integration of the particle concentration and carrier velocity product [3].

The entire process leads to determination of $\epsilon_{th}$ on $\zeta$, which can be plotted as a calibration plot, $\epsilon_{th} = \epsilon_{th}(\zeta)$. Fitting calibration curves to the experimental data leads to the determination of particle magnetic susceptibility for a given range of magnetic susceptibilities. The calibration curve is linear for all Dynabeads $\epsilon_{th}$ ranges but linear only for certain labeled-particle $\epsilon_{th}$ ranges. The linear calibration plot range, $\epsilon_{th} = \epsilon_{th}(\zeta)$, can be approximated using the following equation:

$$\epsilon_{th} = \epsilon_{th}(\zeta) = m\zeta + b \quad (3)$$

where $m$ is the slope, and $b$ is the intercept determined by regression analysis for a set of points in the linear range.

The experimental magnetic susceptibility values for labeled particles, $\Delta\chi_{exp}$, were determined using the following mathematical treatment.

By proper substitution of Eq. (3), we obtained [3]

$$\epsilon_{th} = \epsilon_{th}(\zeta) = m\zeta + b = m\zeta_Q \frac{1}{Q} + b \quad (4)$$

$$\epsilon_{exp} = m_{exp}\zeta_{exp} + b_{exp} = m_{exp}\zeta_{exp}\frac{1}{Q_{exp}} + b_{exp}$$

$$= m'\frac{1}{Q_{exp}} + b_{exp} \quad (5)$$

where the subscript, th, stands for theory and the subscript, exp, is related to the experimental values in magnetapheresis, $Q$ is the volumetric flow-rate, and $\zeta_Q$ is the two-thirds product of $\zeta$, channel width and channel height. Eq. (4) comes from computer simulations of particle trajectories in the magnetic fields using the integration of the particle concentration and carrier velocity profile [3]. Eq. (5) comes from experimental studies. We can obtain the slope $m'$ and intercept $b_{exp}$ by plotting $\epsilon_{exp}$ against $1/Q_{exp}$ on the experimental data points. The following equation must be satisfied in order to fit the theoretical linear regression line to the experimental points.

$$m_{exp} = m,\ \zeta_{exp} = \zeta + (b - b_{exp})/m \quad (6)$$

This equation allows us to plot the experimental data, $\epsilon_{exp}$ and $\zeta_{exp}$, against the theoretical curve, $\epsilon_{th}$ versus $\zeta$. From Eqs. (4), (5) and (6), we can obtain

$$\frac{\Delta\chi_{exp}}{\Delta\chi_t} = \frac{\zeta_{Qexp}}{\zeta_Q},\ \zeta_{Qexp} = \frac{m'}{m} \quad (7)$$

and

$$\Delta\chi_{exp} = \frac{m'}{m} \cdot \frac{\Delta\chi_t}{\zeta_Q} \quad (8)$$

where $\Delta\chi_{exp}$ is the experimentally corrected magnetic susceptibility, $\Delta\chi_t$ is the trial magnetic susceptibility, $m'$ is from Eq. (5), and $m$, $\Delta\chi_t$, $\zeta_Q$ is from the theory. Eq. (6) allows one to plot the experimental data ($\zeta_{exp}$, $\epsilon_{exp}$) against the theoretical curve $\epsilon_{th} = \epsilon_{th}(\zeta)$.

## 3. Experimental

The channel length, breadth, and thickness used were 1.0 cm, 0.1 cm, and 0.025 cm, respectively, the calculated void volume was 0.0025 ml. Analytical

magnetapheresis is a batch type separation technique. Step injections are used in analytical magnetapheresis. The injection volume was equal to 0.02 ml for most experiments and 0.2 ml for Figs. 6 and 7. The particle concentration of the injected sample suspension was $6.0 \cdot 10^4$ particles $ml^{-1}$. Channel components are shown in Fig. 2. The channel consisted of one cut-out layer of Mylar. A thin layer of silicone sealant with embedded 3 μm thick nylon wires was placed between the spacer and a glass plate for easy opening of the channel after magnetapheresis. The layers were then sandwiched between a plastic sheet and a glass plate, which served as the channel walls. The bottom plate, made of thin (150 μm) glass, was used for particle deposition. Finally, all these layers were held together firmly by pressing them evenly with clamps.

Magnetic fields were generated by a permanent magnet assembly consisting of one pair of rare earth magnets (Nd–Fe–B; neodymium–iron–boron) connected by soft-iron pole pieces, which conducted the magnetic flux lines to the interpolar gap. The Nd–Fe–B magnets, characterized by a maximum energy product of $2.39 \cdot 10^5$ T A $m^{-1}$, were obtained from Super Electronics (Taipei, Taiwan). A gap width of 1 mm was used for all experiments, and the gap width corresponded with the deposition boundary. The gap length was 10 cm. The magnetic field measurements were made using a Gaussmeter and a Hall-effect probe (Model Gauss MG-7D, Walker Scientific, Worcester, MA, USA) with adjustable microstages. The probe measured magnetic flux perpendicular to a sensing area with a diameter of 6.94 mm. The combined magnets and pole pieces were 17.5 cm × 10 cm × 6.0 cm and weighed 5.5 kg. The saturation field $B_0$ was 2.8 T. The distance between channel and magnetic gap (shown as $x$ in Fig. 1) was fixed at 0.15 mm for all labeled-particle experiments. Magnetic field strengths were exponentially related to the distance $x$. This distance had to be optimized for particles with high magnetic susceptibilities (such as Dynabeads) at various flow-rates.

Light microscopy (Olympus BX-50, Tokyo, Japan) was used for particle verification. A multichannel syringe pump (Model 200, KD Scientific, Boston, MA, USA) was used for sample and carrier delivery. A hemacytometer was used to count particles exiting at the outlet. Phosphate-buffered saline

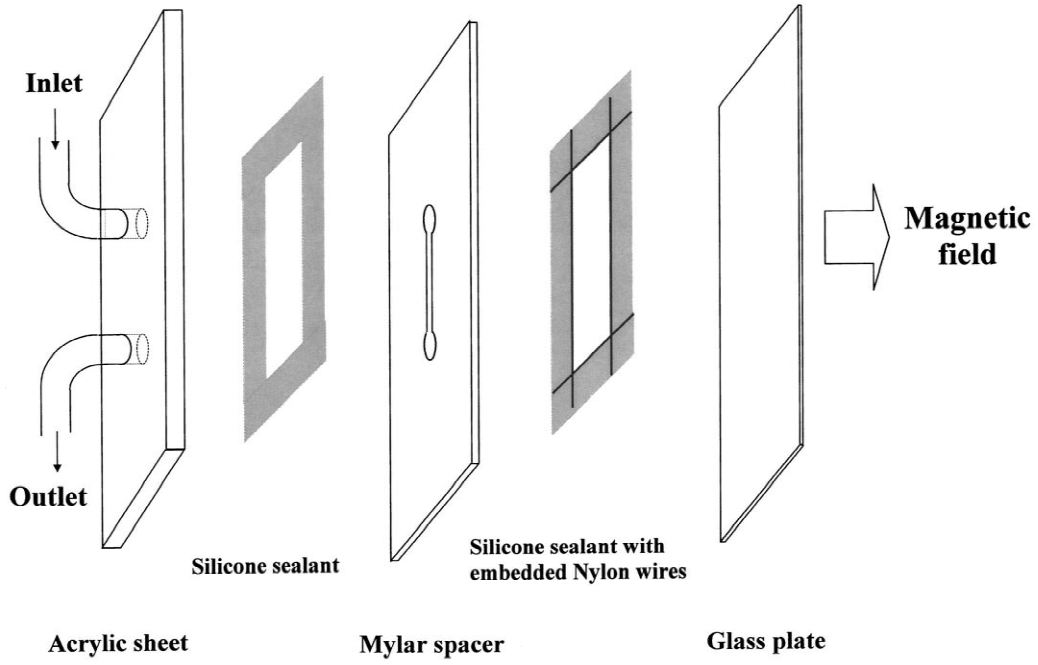


Fig. 2. Channel components of analytical magnetapheresis.

(PBS) solutions and Hank balanced salt (HBS) solutions with pH values of 7.02, viscosities $\eta$ equal to $1.0 \cdot 10^{-3}$ kg m$^{-1}$ s$^{-1}$ were used as carriers in this study. Silica particles (1–5 μm), molybdenum particles (1–5 μm), trypan blue and iron nitrate were purchased from Sigma (St. Louis, MO, USA), erbium chloride was obtained from Strem (Newburyport, MA, USA), 4.5 μm M-450 Dynabeads were obtained from Dynal (Lake Success, NY, USA), copper (II) oxide (1–5 μm), chromium (III) oxide (1–2 μm), tungsten (IV) sulfide (1–2 μm), and iron oxide (1–5 μm) particles were obtained from Aldrich (St. Louis, MO, USA). Yeasts were obtained from a local market, and blood cells were obtained from the Jen-Ai Hospital in Dali (Taichung County, Taiwan).

Various ion labels were prepared by mixing 1 ml of 1 m*M* labeling ions with 9-ml solutions containing fixed numbers of particles for certain time periods and shaking every 15 min. Ion-labeled silicas and yeasts were mixed at room temperature for 1 h, whereas ion-labeled red blood cells (RBCs) were mixed and incubated in ice for 30 min. All ion-labeled particles were washed three times with HBS solution before use to remove unlabeled ions. The labeling ions used in this study were $Er^{3+}$, $Fe^{3+}$, $Mn^{2+}$, $Ni^{2+}$ and $Cu^{2+}$. Deoxy RBCs were prepared by mixing 9-ml solutions containing $2.7 \cdot 10^4$ RBCs with 1 ml of 30 m*M* sodium nitrite at room temperature for 30 min then washing the resulting solutions three times with HBS solution and incubating at 4°C for 1 h before use. Various particle labels were prepared by mixing 1 ml of $7.5 \cdot 10^8$ labeling particles with 9-ml solutions containing approximately $1.0 \cdot 10^5$ samples and incubating at 4°C for 1 h before use. Excess labeling particles were washed and removed as suspensions by centrifugation at 40 *g* for 3 min. Dye exclusion testing was carried out using

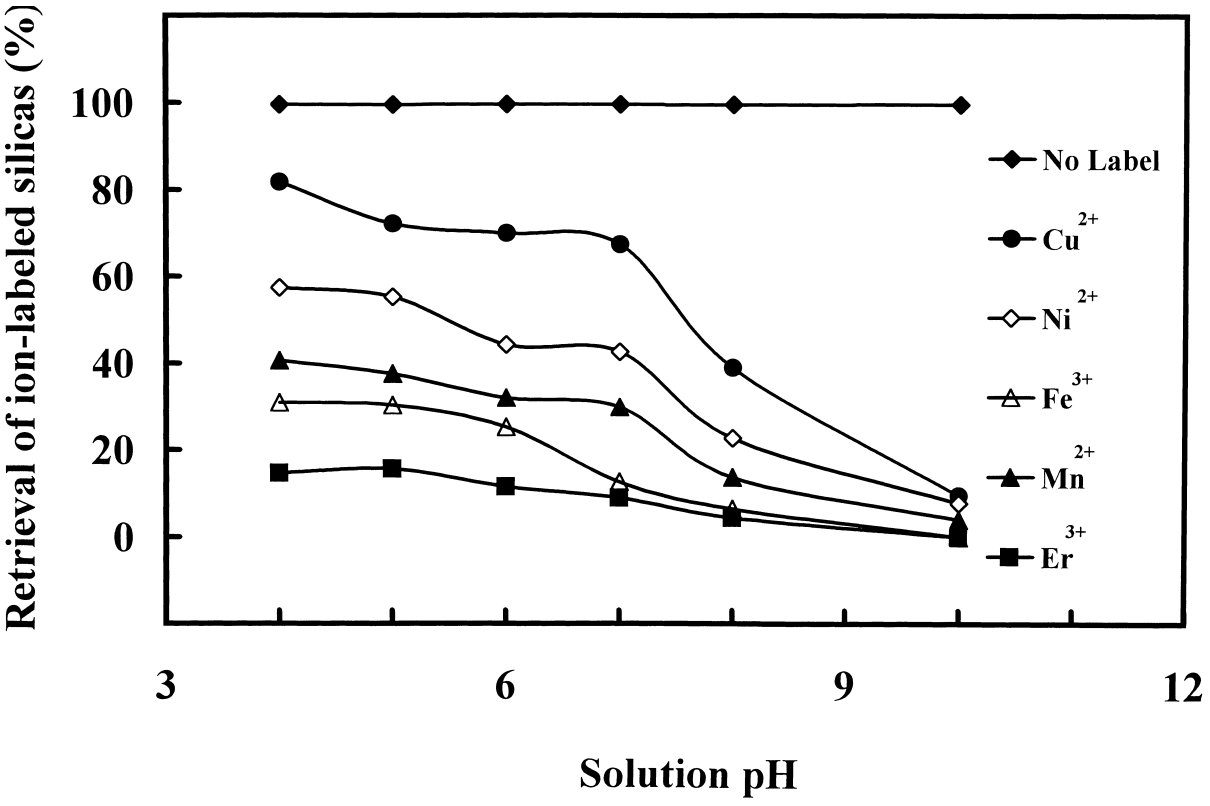


Fig. 3. Solution pH effects on retrievals of ion-labeled silicas in analytical magnetapheresis. The flow velocity was 0.67 mm s$^{-1}$, and an ion concentration of 0.01 m*M* was used for $6.0 \cdot 10^4$ silica labels.

trypan blue stain and a hemacytometer. This method was based on the assumption that viable cells did not take up dyes, whereas nonviable cells did. For viability testing, 0.5 ml containing $1.0 \cdot 10^6$ cell suspensions was mixed thoroughly with 0.5 ml of 0.4% (w/v) trypan blue solution for 5 min before counting.

The minimal numbers of labeled ions per particle required for complete deposition were calculated by dividing the total numbers of ions by the total numbers of particles and assuming complete labeling efficiency. The minimal numbers of particulate labels were directly observed experimentally from the labeled samples and deposition zones using an optical microscope after removal of unlabeled particles.

## 4. Results and discussion

The previously used channel (see Ref. [3]) was constructed using a silicone rubber spacer sandwiched between the top and bottom plates. Channel thickness varied due to compression of the spacer under different pressure forces, and channel leaks occurred from time to time making flow-rates unstable. High pressure forces could avoid channel leaks but would break bottom glass plate easily during channel assembly and disassembly. We replaced the rubber spacer with Mylar to make channel thickness constant, used silicone sealant to sandwich the spacer between the top and bottom plates for a better seal, and employed nylon wires to allow easy disassembly of the bottom plate after magnetapheresis. Silicone sealant can be loosened easily for channel disassembly without breaking bottom glass plate by twisting nylon wires at both ends after magnetapheresis. The channel components are shown in Fig. 2. This improved channel assembly eliminated leakage and could be taken apart easily without breaking the glass plate after experimental testing. The precision of magnetapheresis increased

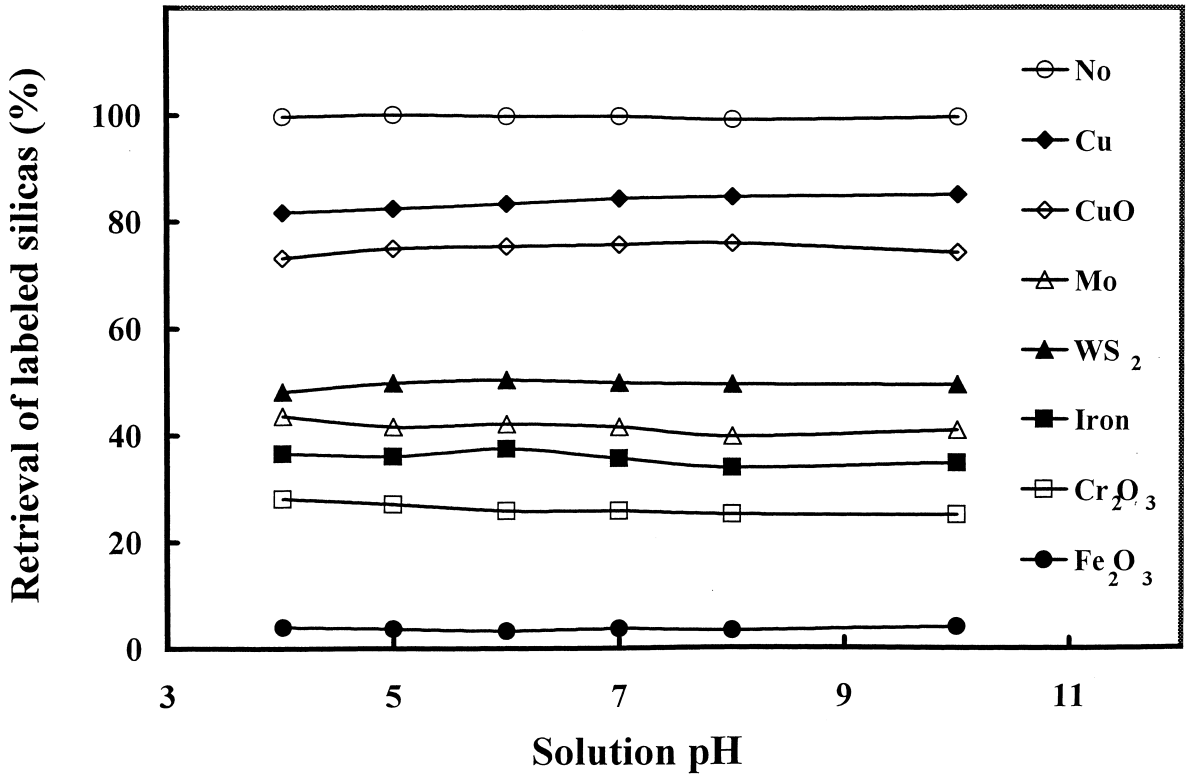


Fig. 4. Solution pH effects on retrievals of particle-labeled silicas in analytical magnetapheresis. The flow velocity was 1.33 mm $s^{-1}$, and there were about one to three particle labels per silica.

remarkably with this improved channel assembly. High linear flow velocities, up to 66.7 mm $s^{-1}$, were used in this improved channel assembly without leakage.

Solution pH effects on the retrieval of ion- and particulate-labeled silicas in analytical magnetapheresis are shown in Figs. 3 and 4. The retrieval of ion-labeled silicas decreased with solution pH, while particulate-labeled silicas were not affected by solution pH. This is consistent with the labeling based on opposite-charge attractions between positively charged ions and the negatively charged silica silanol group at high solution pH. However, the labeling basis of particulate-labeled silica was not dependent on charge attraction so retrievals were not affected significantly by solution pH changes. Fig. 3 shows that the retrieval of ion-labeled silicas changed more significantly with solution pH for less magnetically susceptible ions ($Cu^{2+}$, $Ni^{2+}$) than for more magnetically susceptible ions ($Er^{3+}$).

Solution pH effects on the retrieval of ion-labeled yeasts in analytical magnetapheresis are shown in Fig. 5. Yeast integrity decreased rapidly when solution pH was either greater than 10 or less than 4. The micrographic appearances of the deposition zone when the flow velocity was 3.33 mm $s^{-1}$ for various ion-labeled yeasts are shown in Fig. 6. Deposition-zone areas were roughly consistent with boundaries of channel breadth and interpolar gap widths. Heavier deposits were observed for labeling ions with higher magnetic susceptibilities (e.g., erbium and ferric ions) at fixed flow velocities. The micrographic appearances of the deposition zone for $Fe^{3+}$-labeled silicas with fixed labeling concentration and solution pH at different flow velocities are shown in Fig. 7. Run times varied from 0.38 to 7.50 s. It is clear that depositions increased as flow velocities decreased for $Fe^{3+}$-labeled silicas.

The viabilities of variously labeled red blood cells are shown in Table 1. Molybdenum-labeled cells had lower viabilities than other labeled cells, as shown in Table 1. The magnetic susceptibilities of labeled

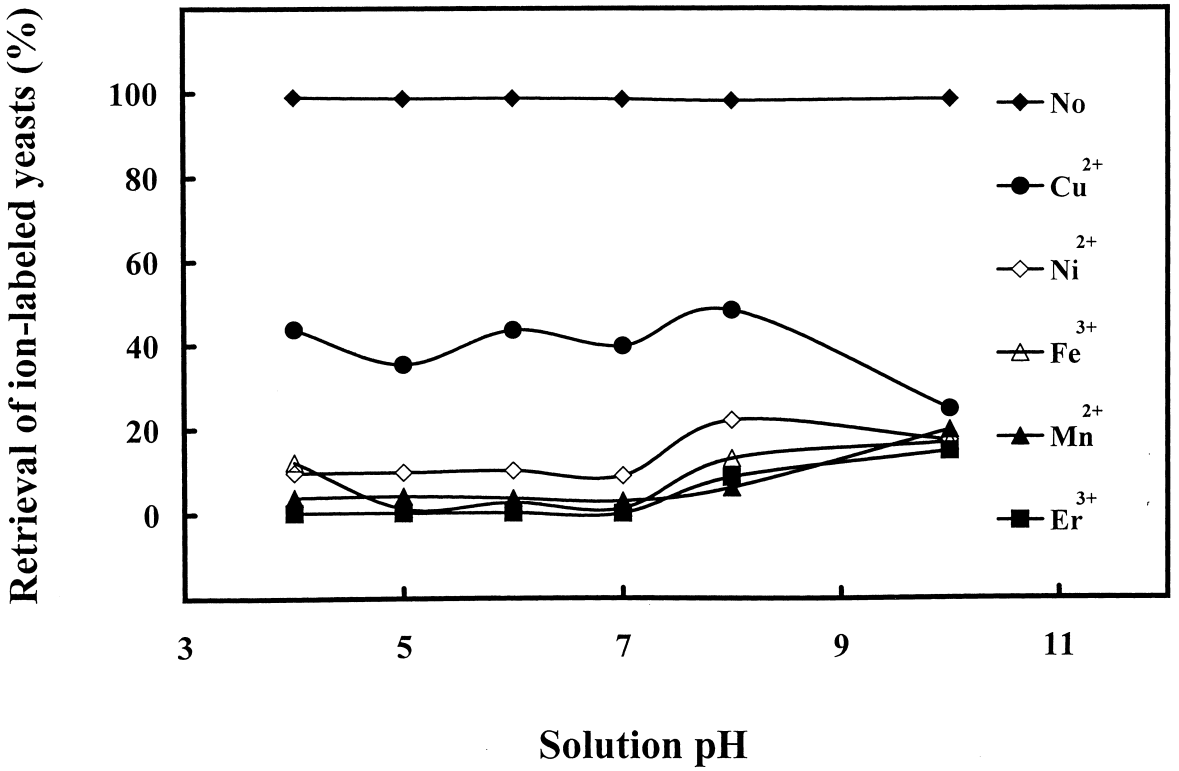


Fig. 5. Solution pH effects on retrievals of ion-labeled yeasts in analytical magnetapheresis. The flow velocity was 3.33 mm $s^{-1}$, and an ion concentration of 0.01 m*M* was used for $6.0 \cdot 10^3$ yeast labels.

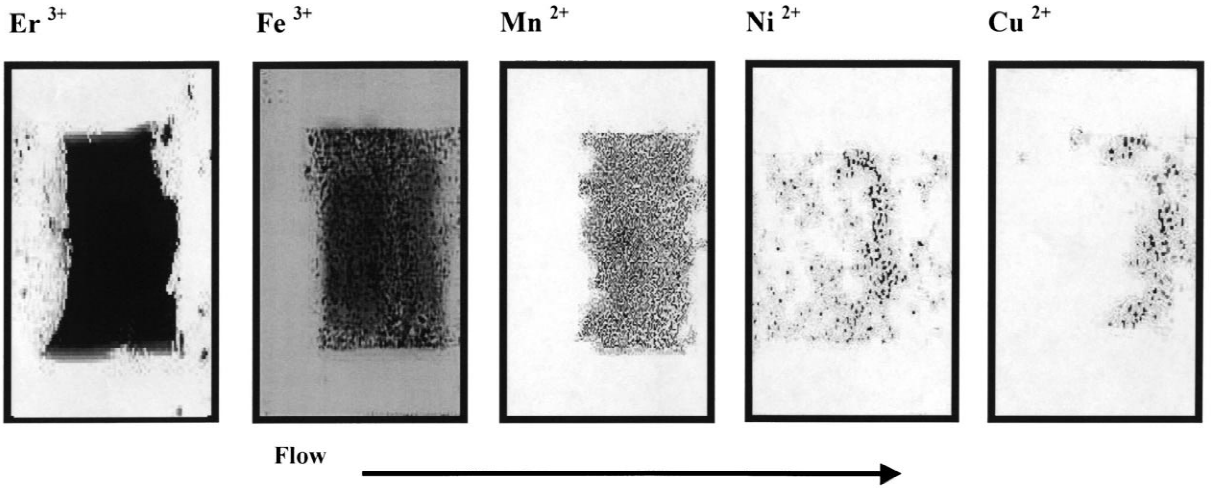


Fig. 6. Microscopic appearances of deposition zone for various ion-labeled yeasts at a flow velocity of 3.33 mm $s^{-1}$. The carrier was PBS with a pH of 7.02.

particles are proportional to the number of magnetic species attached to target particles. The minimal labels of magnetic species per target particle for complete separation would suggest the effective application ranges of analytical magnetapheresis. The minimal concentrations of various labeling ions for complete deposition can be obtained by fixing the flow-rate and progressively decreasing the labeling ion concentration until incomplete deposition appears. The minimal number of labeling ions per particle required for complete deposition in analytical magnetapheresis can be calculated by dividing the number of labeling ions by the number of sample particles. All the ions are assumed to be attached to the particle surface. Labeled particulates were comparable in size to target particles so the labeling results were observed directly using an optical microscope after unlabeled particles were removed. Usually, the ratios were in the range of one to three labeling particles per silica particle. Minimal labeling

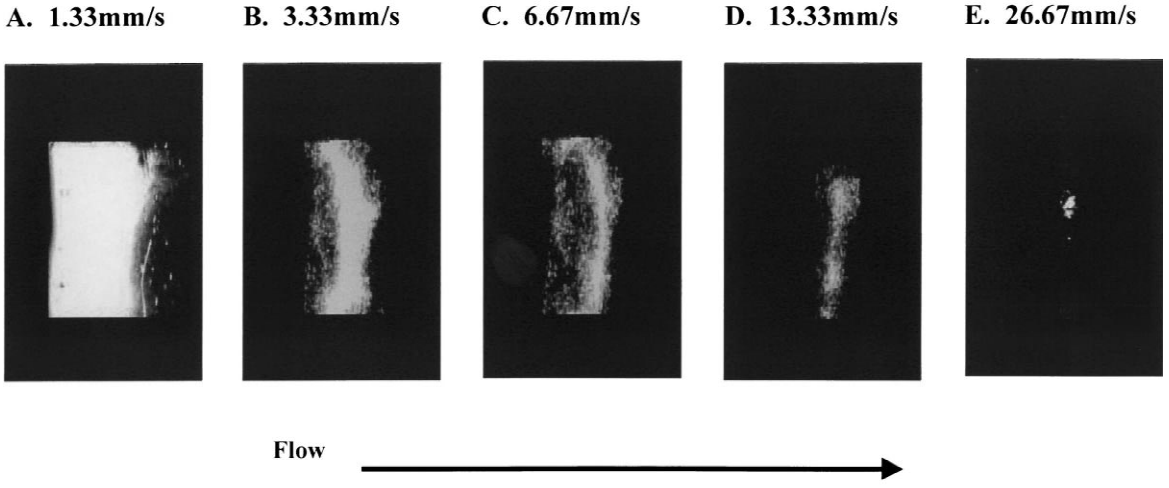


Fig. 7. Microscopic appearances of deposition zone for $Fe^{3+}$-labeled silicas at various flow velocities. An ion concentration of 0.01 m*M* was used for $6.0 \cdot 10^4$ silica labels, and the carrier was PBS with a pH of 7.02.

Table 1
Viability of red blood cells with various labels[a]

| Labeling conditions | Labeling concentration (m$M$) | Percentage of viability ($n=6$) (mean±SD) |
|---|---|---|
| Red blood cells (RBCs) | 0.0 | 100.0±0.0 |
| Deoxy RBCs | | 98.7±0.1 |
| $Er^{3+}$ labeling | 1.0 | 96.7±0.2 |
| $Fe^{3+}$ labeling | 1.0 | 96.3±0.1 |
| $Mn^{2+}$ labeling | 1.0 | 99.3±0.2 |
| $Fe_2O_3$ labeling | 1.0 | 98.0±0.0 |
| Fe labeling | 1.0 | 95.0±0.1 |
| $WS_2$ labeling | 1.0 | 97.7±0.2 |
| Mo labeling | 1.0 | 90.0±0.2 |

[a] SD: Standard deviation. Viability is based on dye exclusion experiments. At least 300 red blood cells were counted in each counting.

concentration results for complete deposition at a flow velocity of 0.67 mm $s^{-1}$ are shown in Table 2. Generally, the number of labeling ions per particle were much higher than when particles were used as labeling reagents. The minimal number of labeling ions per particle required for complete deposition was approximately $2.5\cdot10^{10}$. The actual number of labeling ions may have been lower since labeling efficiency was not completely effective. Table 2 also shows that for highly magnetically susceptible particles, only about one particulate labeling was needed for complete deposition under the same experimental conditions as ion labels.

Overloading occurs when the bottom plate is almost fully covered by the deposited particles. Overloading would play an important role when the total injected particles are over $1.0\cdot10^{6}$ in the present setup. Fortunately, the number of injected particles in this study are at least a 100-times lower than the critical overloading numbers mentioned above. Therefore, overloading does not play an important role in this study.

Determining particle magnetic susceptibilities is another important function of analytical magnetapheresis. The retrieval calibration curves, $\epsilon$, as a function of parameter $\zeta$, for Dynabeads and ion-labeled particles are shown in Fig. 8. A boundary condition for both theoretical curves is $\epsilon=1$ at $\zeta=0$ since this means that at an infinitely high flow velocity ($\zeta=0$) retrieval ($\epsilon$) is equal to 1. The calibration curve was linear for all $\epsilon$ ranges ($0\leq\epsilon\leq1$) of Dynabeads. Most of the data are within 8% error of the theoretical values. The deviations of experimental data from the theoretical values become

Table 2
Minimal number of labels per particle required for complete deposition in analytical magnetapheresis[a]

| Labeling material | Number of labels per silica (mean±SD) | Number of labels per yeast (mean±SD) | Number of labels per RBC (mean±SD) |
|---|---|---|---|
| $Er^{3+}$ | $(3.69\pm0.25)\cdot10^{11}$ | $(2.46\pm0.08)\cdot10^{10}$ | $(2.46\pm0.02)\cdot10^{10}$ |
| $Fe^{3+}$ | $(3.73\pm0.03)\cdot10^{12}$ | $(1.23\pm0.22)\cdot10^{12}$ | $(9.83\pm0.13)\cdot10^{11}$ |
| $Mn^{2+}$ | $(6.30\pm0.11)\cdot10^{14}$ | $(1.23\pm0.18)\cdot10^{13}$ | $(2.46\pm0.02)\cdot10^{13}$ |
| $Ni^{2+}$ | $(2.43\pm0.26)\cdot10^{15}$ | $(2.46\pm0.16)\cdot10^{15}$ | $(6.15\pm0.09)\cdot10^{14}$ |
| $Cu^{2+}$ | $(6.15\pm0.13)\cdot10^{15}$ | $(4.92\pm0.19)\cdot10^{15}$ | $(1.23\pm0.11)\cdot10^{15}$ |
| $Fe_2O_3$ | 1.09±0.56 | 1.17±0.35 | 1.08±0.33 |
| Iron | 1.92±0.35 | 2.73±0.12 | 1.52±0.45 |
| $Cr_2O_3$ | 4.06±0.26 | 4.41±0.21 | 1.58±0.50 |
| CuO | 6.97±0.47 | 3.53±0.32 | 2.26±0.14 |
| Mo | 12.00±0.33 | 14.90±0.55 | 12.0±0.08 |
| $WS_2$ | 16.00±0.45 | 18.76±0.25 | 16.0±0.46 |

[a] SD: Standard deviation. $n=5$.

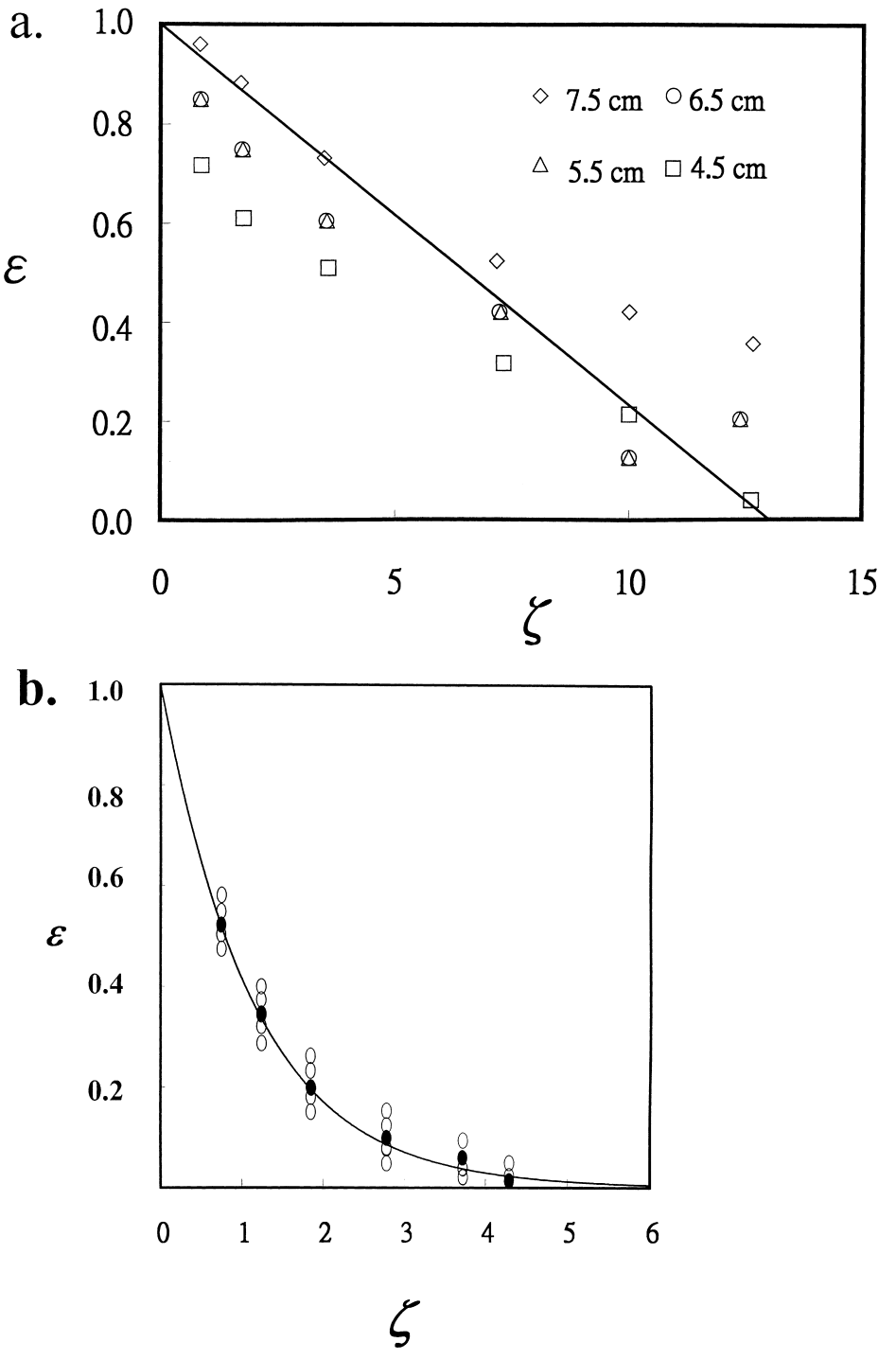


Fig. 8. Retrieval ($\epsilon$) calibration curves as a function of $\zeta$. Solid lines represent theoretical predictions. All discrete data points are averaged values of five measurements. (a) Dynabeads M-450: different distances between channel and interpolar gap were used. The linear equation for data fitting is $y=-0.0758x+1.00$. (b) Erbium ion-labeled particles: open circles represent experimental values, and solid circles were averages for each $\zeta$ value. The linear equation for data fitting in $0<\epsilon<0.3$ is $y=-0.075x+0.339$.

greater for lower $\zeta$ values (high flow-rate) with small (4.5 cm) separation distance (high magnetic field) and high $\zeta$ values (low flow-rate) with large (7.5 cm) separation distance (low magnetic field) in Fig. 8a. This indicates that nonoptimal conditions in flow-rate and magnetic field may contribute to the errors and deserve further study in susceptibility determination of analytical magnetapheresis. Erbium ion-labeled particles were used as examples of the calibration curve for labeled particles, as shown in Fig. 8b. The calibration curve in Fig. 8b was linear only for certain $\epsilon$ ranges ($0<\epsilon<0.3$). The trial magnetic susceptibilities ($\Delta\chi_t$) were 0.245 and $1.0\cdot10^{-6}$ for Dynabeads and labeled particles, respectively. The determined magnetic susceptibilities of Dynabeads M-450 at several separation distances and flow-rates during analytical magnetapheresis were very consistent, as shown in Table 3. The total averaged determination for magnetic susceptibilities for Dynabeads M-450 was 0.25, very close to published value of 0.245 [3]. The same method was used to determine the magnetic susceptibilities of various ion-labeled yeasts and red blood cells, as shown in Tables 4 and 5. Published magnetic susceptibility values were scarce and none were available for comparison with rest of our samplings The measured magnetic susceptibilities of each labeling were very consistent, most were within a 5% variation range.

The new channel assembly in this study eliminated drawbacks found in the previously used channel and better met the needs of analytical magnetapheresis. System characterization, including various labels at different solution pH values and flow-rates were studied. All run times were less than 1 min. The speed and selectivity of analytical magnetapheresis are attractive for many analytical applications, and analytical magnetapheresis can become a useful

Table 3
Determined magnetic susceptibilities of Dynabeads M-450 from analytical magnetapheresis[a]

| Distance between channel and magnetic gap (cm) | Flow-rate (ml min$^{-1}$) | Mean ($\Delta\bar{x}$)±SD ($n=25$) | RSD (%) |
|---|---|---|---|
| 4.5 | 8.0 | | |
| | 4.0 | | |
| | 2.0 | 0.25±0.01 | 4.0 |
| | 1.0 | | |
| | 0.6 | | |
| 5.5 | 8.0 | | |
| | 4.0 | | |
| | 2.0 | 0.25±0.01 | 4.0 |
| | 1.0 | | |
| | 0.6 | | |
| 6.5 | 8.0 | | |
| | 4.0 | | |
| | 2.0 | 0.25±0.01 | 4.0 |
| | 1.0 | | |
| | 0.6 | | |
| 7.5 | 8.0 | | |
| | 4.0 | | |
| | 2.0 | 0.24±0.01 | 4.1 |
| | 1.0 | | |
| | 0.6 | | |

[a] SD: Standard deviation, RSD: relative standard deviation.

Table 4
Determined magnetic susceptibilities of yeasts with various ion labels from analytical magnetapheresis[a]

| Labeling ion | Flow-rate (ml min$^{-1}$) | Mean ($\Delta\bar{x}$)±SD·$10^6$ ($n=25$) | RSD (%) |
|---|---|---|---|
| $Er^{3+}$ | 0.40 | | |
| | 0.20 | | |
| | 0.10 | 27.92±1.14 | 4.1 |
| | 0.05 | | |
| | 0.02 | | |
| $Fe^{3+}$ | 0.40 | | |
| | 0.20 | | |
| | 0.10 | 22.7±1.4 | 6.0 |
| | 0.05 | | |
| | 0.02 | | |
| $Mn^{2+}$ | 0.40 | | |
| | 0.20 | | |
| | 0.10 | 7.09±0.47 | 6.6 |
| | 0.05 | | |
| | 0.02 | | |
| $Ni^{2+}$ | 0.40 | | |
| | 0.20 | | |
| | 0.10 | 5.98±0.50 | 8.3 |
| | 0.05 | | |
| | 0.02 | | |
| $Cu^{2+}$ | 0.40 | | |
| | 0.20 | | |
| | 0.10 | 3.12±0.10 | 3.3 |
| | 0.05 | | |
| | 0.02 | | |

[a] SD: Standard deviation, RSD: relative standard deviation.

Table 5
Determined magnetic susceptibilities of red blood cells (RBCs) with various ion labels from analytical magnetapheresis[a]

| Flow-rate (ml min$^{-1}$) | RBCs $\Delta\chi\cdot10^6$ | Deoxy RBCs $\Delta\chi\cdot10^6$ | Labeling ion | | | | |
|---|---|---|---|---|---|---|---|
| | | | $Er^{3+}$ $\Delta\chi\cdot10^6$ | $Fe^{3+}$ $\Delta\chi\cdot10^6$ | $Mn^{2+}$ $\Delta\chi\cdot10^6$ | $Ni^{2+}$ $\Delta\chi\cdot10^6$ | $Cu^{2+}$ $\Delta\chi\cdot10^6$ |
| 0.40 | 1.037 | 2.082 | 27.092 | 14.678 | 8.799 | 3.267 | 2.939 |
| 0.20 | 1.066 | 1.877 | 27.412 | 12.897 | 8.392 | 3.369 | 2.801 |
| 0.10 | 1.043 | 2.048 | 27.351 | 14.898 | 8.921 | 3.456 | 2.921 |
| 0.05 | 1.056 | 1.988 | 27.244 | 14.268 | 8.294 | 3.269 | 2.937 |
| 0.02 | 1.039 | 2.157 | 27.132 | 14.986 | 8.403 | 3.059 | 2.629 |
| Mean ($\bar{x}$)±SD ($n$=25) | 1.05±0.01 | 2.03±0.10 | 27.35±0.14 | 14.75±0.26 | 8.56±0.28 | 3.28±0.14 | 2.85±0.13 |
| RSD (%) | 1.0 | 4.9 | 0.5 | 1.8 | 3.3 | 4.3 | 4.6 |

[a] SD: Standard deviation, RSD: relative standard deviation.

technique for analyzing magnetically susceptible particles.

## Acknowledgements

This work was supported by the National Science Council of Taiwan, Republic of China (NSC-88-2113-M-324-003). Thanks to the Jen-Ai Hospital of Dali in Taichung, Taiwan for providing blood cell samples.

## References

[1] R. Mitchell, D.W. Bitton, J.A. Oberteuffer, Sep. Purif. Methods 4 (1975) 267.
[2] T. Yalcin, Int. J. Mineral Process. 34 (1992) 119.
[3] M. Zborowski, C.B. Fuh, R. Green, L. Sun, J.J. Chalmers, Anal. Chem. 67 (1995) 3702.
[4] J.P. Hancock, J.T. Kemshed, J. Immunol. Methods 164 (1993) 51.
[5] S. Funderud, K. Nustad, T. Lea, F. Vartdal, G. Guadernack, P. Stensted, L. Ugelstad, in: G.B. Klaus (Ed.), Lymphocytes – A Practical Approach, Oxford University Press, New York, 1987, pp. 55–61.
[6] J. Ugelstad, P. Stensted, L. Kilaas, W.S. Prestvik, R. Herje, A. Berge, E. Hornes, Blood Purif. 11 (1993) 347.
[7] R. Tyagi, M.N. Gupta, Biotech. Appl. Biochem. 21 (1995) 217.
[8] Y. Morimoto, H. Nattsume, Japan. J. Clin. Med. 56 (1998) 649.
[9] C.M. Schweitzer, C.E. van der Schoot, A.M. Drager, P. van der Valk, A. Zevenbergen, B. Hooibrink, A.H. Westra, M.M. Langenhuijsen, Exp. Hematol. 23 (1995) 41.
[10] A.F.M. van Velsen, G. van der Vos, R. Boersma, J.L. de Reuver, Water Sci. Technol. Proc. IAWPRC Int. Conf. 24 (1991) 195.
[11] Y. Sakai, F. Takahash, T. Miama, Water Res. 31 (1997) 2113.
[12] C.B. Fuh, S.Y. Chen, J. Chromatogr. A 813 (1998) 313.